JCB Article

ERK activation promotes neuronal degeneration predominantly through plasma membrane damage and independently of caspase-3

Srinivasa Subramaniam,[1] Ute Zirrgiebel,[2] Oliver von Bohlen und Halbach,[1] Jens Strelau,[1] Christine Laliberté,[4] David R. Kaplan,[3,4] and Klaus Unsicker[1]

[1]Neuroanatomy and Interdisciplinary Center for Neurosciences, University of Heidelberg, D-69120 Heidelberg, Germany
[2]Montreal Neurological Institute, Montreal, Quebec H3A 2B4, Canada
[3]Department of Medical Genetics and Microbiology and Institute of Medical Sciences, University of Toronto, Toronto, Ontario M5S 1A8, Canada
[4]The Hospital for Sick Children, Toronto, Ontario M5G 1X8, Canada

Our recent studies have shown that extracellular-regulated protein kinase (ERK) promotes cell death in cerebellar granule neurons (CGN) cultured in low potassium. Here we report that the "death" phenotypes of CGN after potassium withdrawal are heterogeneous, allowing the distinction between plasma membrane (PM)–, DNA-, and PM/DNA-damaged populations. These damaged neurons display nuclear condensation that precedes PM or DNA damage. Inhibition of ERK activation either by U0126 or by dominant-negative mitogen-activated protein kinase/ERK kinase (MEK) overexpression results in a dramatic reduction of PM damaged neurons and nuclear condensation. In contrast, overexpression of constitutively active MEK potentiates PM damage and nuclear condensation. ERK-promoted cellular damage is independent of caspase-3. Persistent active ERK translocates to the nucleus, whereas caspase-3 remains in the cytoplasm. Antioxidants that reduced ERK activation and PM damage showed no effect on caspase-3 activation or DNA damage. These data identify ERK as an important executor of neuronal damage involving a caspase-3–independent mechanism.

Introduction

Neural cells die in large numbers during development, and thereby significantly shape the developing brain (Oppenheim, 1991). In the adult brain, both acute lesions and chronic neurodegenerative diseases go along with cell death (Nijhawan et al., 2000). Two types of neuron death are generally considered to be distinguishable. Acute oxidative stress and injury can cause necrosis, whereas apoptotic cell death can be induced by growth factor withdrawal and extracellular death signals (Martin, 2001). There is growing evidence to support the notion that neuronal death can result from varying contributions of coexisting apoptotic and necrotic mechanisms (Martin, 2001). Thus, a picture is beginning to emerge suggesting an apoptosis–necrosis cell death continuum. However, the molecular bases generating this continuum are still not understood.

Although defined molecular entities that can promote necrotic cell death are beginning to emerge (Wang, 2000), molecular players that promote apoptosis have been more extensively studied. A group of cysteine proteases termed caspases has been proposed as a major executor of apoptotic cell death that is accompanied by nuclear condensation and internucleosomal DNA fragmentation (Hengartner, 2000). Caspase-3, a pro-enzyme (composed of a short NH_2-terminal pro-domain followed by p17 and p21 subunits), is cleaved to yield the p17 active fragment upon a cell death stimulus

The online version of this article includes supplemental material.

Address correspondence to S. Subramaniam, Neuroanatomy and Interdisciplinary Center for Neurosciences, University of Heidelberg, Im Neuenheimer Feld 307, 2. OG, D-69120 Heidelberg, Germany. Tel.: 49 6221 54 8304. Fax: 49 6221 54 5604.
email: Srinivasa.Subramaniam@urz.uni-heidelberg.de

Key words: DNA damage; apoptosis; necrosis; MAPK; antioxidants

Abbreviations used in this paper: Ac-DEVD-CHO, acetyl-Asp-Glu-Val-Asp-aldehyde; CA, constitutively active; CGN, cerebellar granule neuron; CHX, cyclohexamide; CN, condensed nuclei; DN, dominant-negative; Egr-1, early growth response gene-1; ERK, extracellular-regulated protein kinase; JNK, c-Jun NH2-terminal kinase; MEK, MAPK/ERK kinase; MOI, multiplicity of infection; N-AC, N-acetyl cysteine; pERK, persistent active ERK; PI, propidium iodide; PM, plasma membrane; ROS, reactive oxygen species; SOD, superoxide dismutase; Z-VAD-FMK, benzyloxy-carbonyl-Val-Ala-Asp-fluoromethylketone.

© The Rockefeller University Press, 0021-9525/2004/05/357/13 $8.00

(Nicholson et al., 1995). The p17 fragment has been shown to cleave the inhibitor of the endonuclease caspase-activated DNase, leading to caspase-activated DNase activation and resulting in DNA damage (Enari et al., 1998).

Cerebellar granule neurons (CGN) from postnatal rat provide an excellent system to study neuronal cell death. CGN survive for weeks in vitro and develop characteristics of mature CGN when maintained in depolarizing concentrations of K^+ (25 mM) but undergo cell death when cultured in low K^+ (5 mM) conditions (D'Mello et al., 1993). Although mechanisms underlying CGN death are not yet fully understood, a requirement of RNA/protein synthesis, generation of reactive oxygen species (ROS), activation of caspases, and phosphorylation of c-Jun have been implicated in this cell death model (Schulz et al., 1996; Watson et al., 1998).

The MAPKs are serine/threonine protein kinases, which play pivotal roles in a variety of cell functions in many cell types (Davis, 1993). Three major mammalian MAPK subfamilies have been described: the extracellular-regulated protein kinases (ERKs), the c-Jun NH_2-terminal kinases (JNK), and the p38 kinases. Each MAPK is activated by a specific phosphorylation cascade. The best characterized ERK pathway involves the activation of Ras at the plasma membrane (PM) and the sequential activation of a series of protein kinases. Initially, Ras interacts with and activates Raf-1, which in turn activates MAPK/ERK kinase (MEK)-1 and -2 by serine phosphorylation. MEK1/2 then catalyze the phosphorylation of ERK-1 and -2 on tyrosine and threonine residues, and these activated MAPKs can phosphorylate cytoplasmic or nuclear targets.

Although activation of ERK by some conditions of stress, particularly oxidant injury, or by growth factors is believed to confer a survival advantage to cells (Xia et al., 1995; Guyton et al., 1996; Wang et al., 1998), a death-promoting role of ERK has become increasingly clear recently in both in vitro and in vivo models of neuronal death. H_2O_2-induced ERK induction in an oligodendrocyte cell line was implicated in cell death (Bhat and Zhang, 1999). In primary neuronal cells, glutamate- or camptothecin-induced neuronal injury was shown to require ERK activation (Stanciu et al., 2000; Lesuisse and Martin, 2002). In addition, inhibition of ERK activation protects against cell damage resulting from focal cerebral ischemia (Alessandrini et al., 1999; Namura et al., 2001; Noshita et al., 2002). These papers highlight a potentially detrimental role of ERK signaling. However, the molecular mechanisms orchestrated by ERK to promote cellular demise are not yet clear. We have recently shown that death of CGN in low K^+ is accompanied by a sustained activation of ERK. Inhibition of persistent active ERK (pERK) with specific inhibitors resulted in a decrease in c-Jun activation as well as a decrease in cell death (Subramaniam et al., 2003).

In an attempt to further explore the mechanistic basis of ERK-promoted neuronal death, we report the following major findings: (a) CGN die by exhibiting features of PM, DNA, and PM/DNA damage; (b) ERK is predominantly involved in the execution of PM but not DNA damage–mediated cell death; (c) the cell death–promoting effect of ERK is independent of caspase-3; (d) pERK translocates to the nucleus, whereas caspase-3 remains in the cytoplasm of the dying neurons; and (e) ERK activation is down-regulated by antioxidants and protein synthesis inhibitor.

Results

Low potassium triggers PM and DNA damage in CGN

CGN are dependent on depolarizing concentrations of potassium (25–30 mM) for their survival and differentiation. Changing the high concentration of potassium to a low concentration (5 mM) induces cell death. We used three established markers for monitoring cellular damage, propidium iodide (PI) to monitor PM damage, enzymatic TUNEL staining to monitor DNA damage, and DAPI staining to monitor morphological changes of nuclei (see Materials and methods).

3 h after switching to low potassium, <2% of the neurons were PI or TUNEL positive. 5 ± 1% of the neurons were both TUNEL and PI positive (Fig. 1, A and B). At 6 h, a slight but significant increase in the percentages of cells that were exclusively PI or TUNEL positive was noted. By 12 h, the number of TUNEL-stained neurons (21 ± 1%) was slightly larger than that of the PI-positive (12 ± 1%) neurons. However, at 24 h the number of PI-positive neurons (31 ± 2%) exceeded that of TUNEL-stained neurons (20 ± 1%). At this point, neurons displaying both TUNEL and PI staining had increased compared with 12 h (13 ± 1 vs. 5 ± 1%). At 48 h, exclusively PI-positive neurons (42 ± 2%) clearly exceeded the percentage of exclusively TUNEL-positive neurons (17 ± 2%). A significant increase in the neuronal population positive for both PI and TUNEL (22 ± 1%) occurred at 48 h (Fig. 1 B).

All three neuronal subpopulations characterized by PI, TUNEL, and TUNEL plus PI staining shown in Fig. 1 C (asterisk, arrow, and arrowhead, respectively) displayed nuclear shrinkage (condensation) in a DAPI-stained specimen. Measurements of nuclear size showed significant differences between the PI only, TUNEL only, and TUNEL plus PI groups (Fig. 1 D). The mean nuclear diameter of PI-positive neurons (20.66 ± 0.81 μm^2) was significantly larger ($P < 0.001$) than that of the TUNEL-stained neurons (13.09 ± 0.42 μm^2) or cells stained for both PI and TUNEL (13.81 ± 0.81 μm^2). Undamaged neurons (TUNEL−/PI−) showed nuclear diameters of 27.65 ± 1.20 μm^2.

Together, these results suggest that (a) PI staining indicating PM and DNA damage identified by TUNEL staining occurs in partly distinct and partly overlapping subsets of neurons as early as 6 h after potassium deprivation, (b) by 48 h the fraction of neurons with only PM damage is larger than the other two neuronal subpopulations, and (c) the PM-damaged neurons have comparatively larger nuclei than the DNA-damaged neurons.

ERK activation is a prerequisite for PM damage

Active ERK1/2 contributes to death of CGN induced by low potassium because inhibition of ERK1/2 activation prevents CGN death (Subramaniam et al., 2003). The effect of ERK1/2 inhibition on the aforementioned neuronal subpopulation was analyzed using the MEK1/2 inhibitor U0126 (20 μM). U0126 was added to low potassium CGN

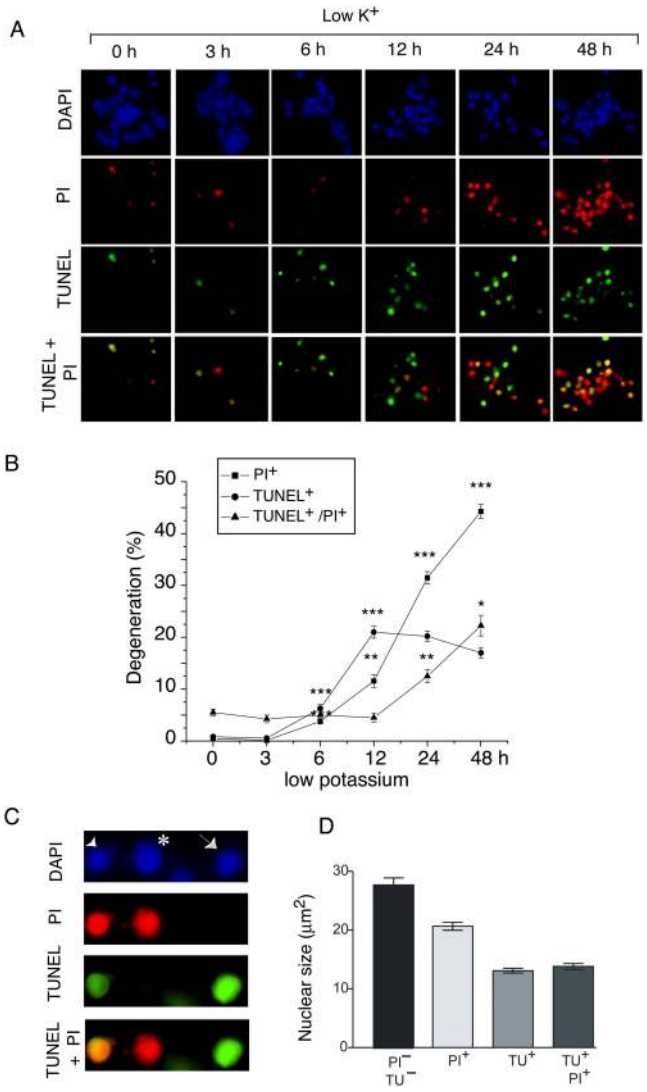

Figure 1. **Low potassium triggers PM and DNA damage in CGN.** After potassium change (low K^+), the CGN were triple stained (see Materials and methods). (A) Photomicrographs of PI- (PM damaged), TUNEL- (DNA damaged), and TUNEL + PI (DNA and PM damaged)–stained neurons and their corresponding DAPI stain. (B) Quantification of PI+ (PM damaged only), TUNEL+ (DNA damaged only), and TUNEL+/ PI+ (both DNA and PM damaged) neurons are given as a percent of the total number of DAPI-stained neurons. (C) Nuclear morphologies of damaged neurons; asterisk, only PM damaged; arrow, only DNA damaged; arrowhead, both DNA and PM damaged. (D) Nuclear size of the damaged neurons at 24 h after low K^+ change as measured by DAPI-stained nuclei. PI+, only PM damaged; TUNEL+, only DNA damaged; TUNEL+/PI+, both DNA and PM damaged; TUNEL−/PI−, neither DNA nor PM damaged. Error bars represent mean ± SEM from at least three experiments. ***$P < 0.001$, **$P < 0.01$, and *$P < 0.05$ as compared with the previous time point (e.g., *$P < 0.05$ at 48 h is compared with 24 h).

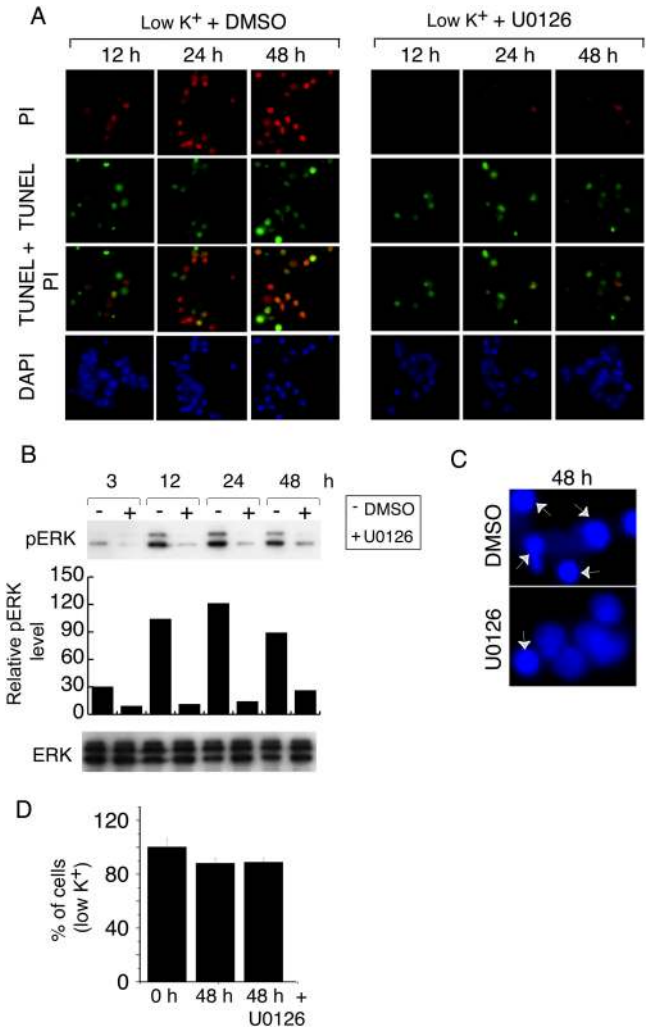

Figure 2. **Sustained ERK activation is required for cellular damage.** (A) Photomicrographs of cells treated with 20 μM U0126 and vehicle (DMSO, 0.1%) for 12, 24, and 48 h after potassium change. (B) Western blot analysis showing sustained ERK activation and its attenuation by U1026. (C) DAPI-stained neurons. CN (arrows) in the presence of U0126 or DMSO at 48 h. (D) Percentage of total DAPI cells in control and in U0126-treated culture.

cultures for 6, 12, 24, and 48 h, and cultures were exposed to PI and stained with TUNEL and DAPI. U0126 prevented the increase in PI-stained neurons at all the time points analyzed (Fig. 2 A and Table I), suggesting an active role of ERK in the execution of PM damage. U0126 also significantly decreased numbers of TUNEL-positive neurons at 6, 12, and 24 h. However, at 48 h numbers of TUNEL-positive neurons were no longer significantly different from those in inhibitor-untreated cultures (Table I), suggesting that ERK inhibition clearly decreased cell death mediated by PM damage but failed to provide robust and persistent protection of cells dying by DNA damage. Numbers of neurons exhibiting signs of both DNA and PM damage were also significantly decreased by U0126.

The nuclear condensation data (Table I) indicate that, although the U0126 had an early effect (6 and 12 h) on decreasing the number of neurons with condensed nuclei (CN), which are PI-negative, U0126 had a robust effect on decreasing the CN of PI-positive cells for all time points analyzed. This further characterizes ERK as an inducer of nuclear condensation that is predominantly associated with PM damage. Fig. 2 C represents the photomicrograph of the DAPI-stained cells in U0126- and DMSO-treated culture, showing the nuclear condensation (arrows). U0126 clearly attenuated ERK1/2 activation at all time points analyzed (Fig. 2 B). A total loss of ~10% of cells both in untreated

Table I. **ERK activation promotes PM damage and nuclear condensation**

	DMSO					U0126				
Low K^+	**PI+**	**TUNEL+**	**TUNEL+/PI+**	**CN/PI+**	**CN/PI−**	**PI+**	**TUNEL+**	**TUNEL+/PI+**	**CN/PI+**	**CN/PI−**
h	%	%	%	%	%	%	%	%	%	%
6	4 ± 1	6 ± 1	4 ± 1	8 ± 2	23 ± 3	2 ± 1	3 ± 1	5 ± 1	7 ± 1	6 ± 1[a]
12	12 ± 1	19 ± 1	5 ± 1	17 ± 1	20 ± 1	4 ± 1[a]	10 ± 1[a]	6 ± 1	11 ± 2[a]	10 ± 1[a]
24	31 ± 2	21 ± 1	12 ± 1	44 ± 1	21 ± 3	13 ± 1[a]	14 ± 1	7 ± 1[b]	18 ± 2[a]	15 ± 2
48	41 ± 2	16 ± 2	22 ± 3	63 ± 2	16 ± 1	12 ± 1[a]	21 ± 1	14 ± 2[c]	23 ± 1[a]	14 ± 1

At the time of potassium change (low K^+), U0126 (20 μM) or DMSO (0.1%) was added for 6, 12, 24, and 48 h, and triple staining was performed. Data are given as a percentage of the total number of PI+, TUNEL+, and TUNEL+/PI+ neurons. Percentage of total neurons with condensed nuclei (CN), which are PI+ and PI−, are also given.
[a]$P < 0.001$ compared with DMSO treatment.
[b]$P < 0.01$ compared with DMSO treatment.
[c]$P < 0.05$ compared with DMSO treatment.

and U0126-treated cultures was observed at 48 h (Fig. 2 D), suggesting that the U0126 treatment, per se, did not result in an apparent loss of cells from the culture plate.

In addition, data in Table II demonstrate that at 6 h in low potassium ~17% of neurons were neither TUNEL positive nor PI positive but exhibited nuclear condensation (CN/PI−/TUNEL−), supporting the notion that nuclear condensation precedes DNA or PM damage. However, at later time points the total percentage of CN was smaller or equaled the total percentage of damaged cells. This finding may be due to a fast and irreversible commitment of neurons to die around ~12 h after the potassium switch (Miller and Johnson, 1996). The role of JNK and p38 (the other two members of MAPK pathway) in PM damage was analyzed. The JNK inhibitor, JNKI1, had a small but significant effect on decreasing PM damage, but p38 inhibitor SB203580 had no apparent effect on PM damage (Fig. S1, available at http://www.jcb.org/cgi/content/full/jcb.200403028/DC1).

The effect of overexpression of DN MEK and CA MEK in CGN

CGN were infected with recombinant adenovirus expressing dominant-negative (DN) MEK, constitutively active (CA) MEK, and GFP. The proportion of CGN exhibiting both PM damage and CN in Ad-DN MEK (350 multiplicity of infection [MOI])–infected cultures was significantly ($^{\circ\circ}P < 0.01$) lower than the proportion of such neurons in Ad-GFP–infected cultures (Fig. 3, A and B). Although ~65% of the total Ad-GFP–infected neurons exhibited signs of cellular damage, only ~17% of the total Ad-DN MEK–infected neurons showed cellular damage. DN MEK overexpression markedly inhibited ERK1/2 activation observed in GFP-infected (control) cultures (Fig. 3 C). Therefore, an inhibition of the ERK pathway by pharmacological treatment or by using Ad-DN MEK can prevent cellular damage, further substantiating the role of the MEK–ERK pathway in neuronal degeneration.

The effect of CA MEK overexpression in CGN was tested using Ad-CA MEK at 350 MOI. Interestingly, a dramatic increase in PM-damaged neurons was observed in Ad-CA MEK–infected as compared with Ad-GFP–infected cultures (Fig. 3 A; and Fig. 3 B, $^{**}P < 0.01$). Around 85% of the Ad-CA MEK–infected neurons were positive for PM damage. >80% of the Ad-CA MEK–infected neurons displayed nuclear condensation. CA MEK overexpression-induced ERK activation is evident at 3 h in low potassium cultures (Fig. 3 D). At 12 h, Ad-CA MEK overexpression significantly increased ERK1/2 phosphorylation compared with control cultures (Fig. 3 D). At 24 h, ERK1/2 phosphorylation in Ad-CA MEK–infected CGN culture was reduced compared with control cultures (unpublished data). This occurrence is possibly due to the dramatically accelerated cell death in Ad-CA MEK–infected neurons that may result in an overall decrease in phosphorylation of ERK (unpublished data). These data suggest that Ad-CA MEK overexpression enhances cellular damage of CGN maintained in low potassium, apparently by increasing the level of ERK activation. The viral expression for Ad-GFP, Ad-DN MEK, and Ad-CA MEK (all at 350 MOI) did not result in apparent toxicity (Fig. 3 E).

Degeneration promoted by ERK is independent of caspase-3

We first assayed for an effect of acetyl-Asp-Glu-Val-Asp-aldehyde (Ac-DEVD-CHO), a selective inhibitor of caspase-3. Ac-DEVD-CHO (100 μM) efficiently prevented DNA

Table II. **Nuclear condensation precedes PM or DNA damage**

Low K^+	**CN**	**CN/PI+/TUNEL−**	**CN/PI−/TUNEL+**	**CN/PI+/TUNEL+**	**CN/PI−/TUNEL−**
h	%	%	%	%	%
6	31 ± 2	4 ± 1	6 ± 1	4 ± 2	17 ± 2
12	37 ± 2	12 ± 2	19 ± 1	5 ± 1	2 ± 1
24	64 ± 2	31 ± 2	21 ± 1	12 ± 1	2 ± 1

Percentage of total number of CN, which are damaged only for PM (CN/PI+/TUNEL−), or DNA (CN/PI−/TUNEL+), or both (CN/PI+/TUNEL+). CN/PI−/TUNEL− condensed neurons neither PM nor DNA damaged.

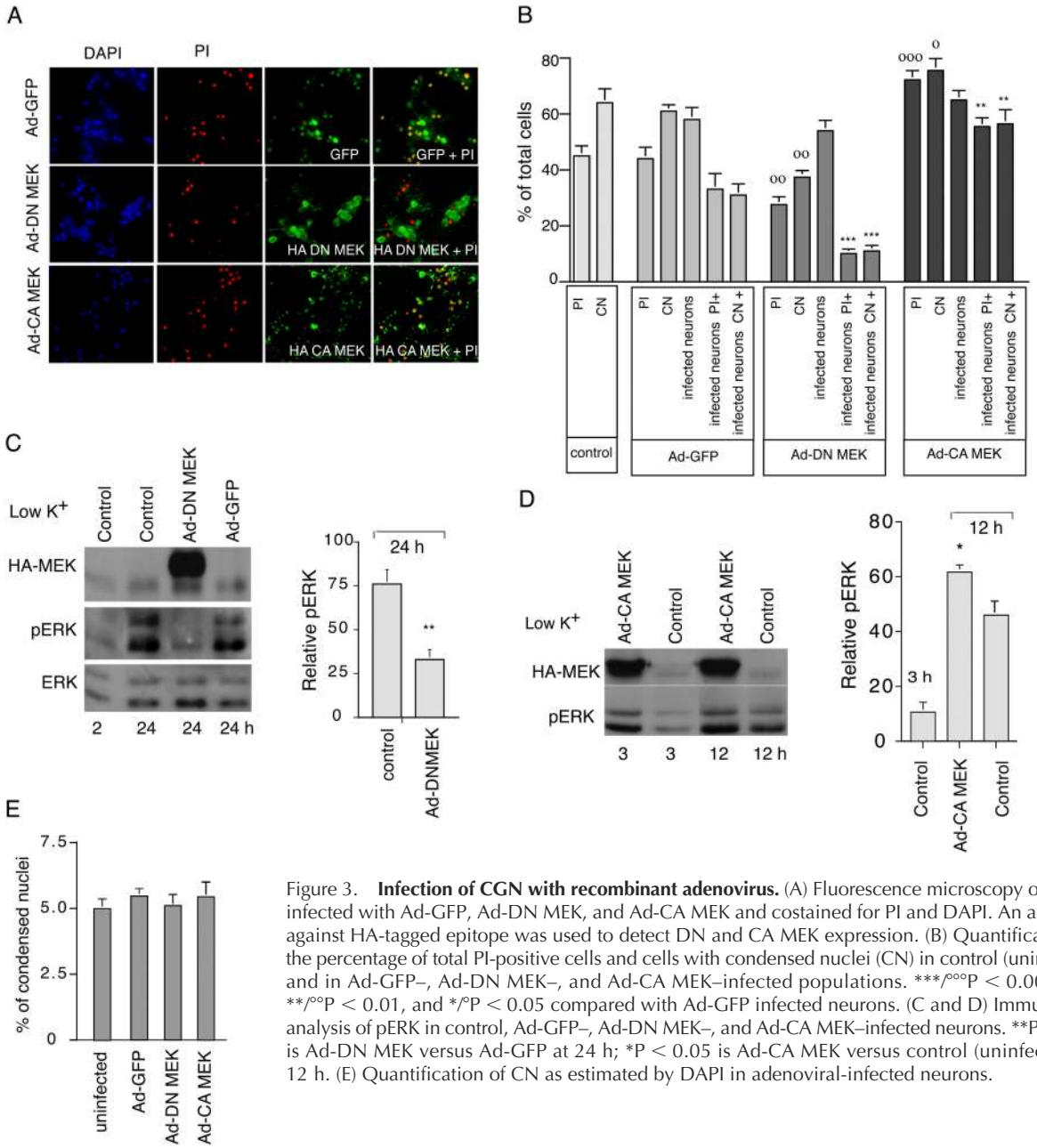

Figure 3. **Infection of CGN with recombinant adenovirus.** (A) Fluorescence microscopy of CGN infected with Ad-GFP, Ad-DN MEK, and Ad-CA MEK and costained for PI and DAPI. An antibody against HA-tagged epitope was used to detect DN and CA MEK expression. (B) Quantification of the percentage of total PI-positive cells and cells with condensed nuclei (CN) in control (uninfected) and in Ad-GFP–, Ad-DN MEK–, and Ad-CA MEK–infected populations. ***/°°°$P < 0.001$, **/°°$P < 0.01$, and */°$P < 0.05$ compared with Ad-GFP infected neurons. (C and D) Immunoblot analysis of pERK in control, Ad-GFP–, Ad-DN MEK–, and Ad-CA MEK–infected neurons. **$P < 0.01$ is Ad-DN MEK versus Ad-GFP at 24 h; *$P < 0.05$ is Ad-CA MEK versus control (uninfected) at 12 h. (E) Quantification of CN as estimated by DAPI in adenoviral-infected neurons.

damage and condensation of nuclei but failed to prevent PI uptake, suggesting an involvement of a caspase-3–independent mechanisms in neuronal PM damage (Fig. 4 A). This observation is in line with a previous paper (D'Mello et al., 2000) showing that potassium-deprived CGN cultured from caspase-3 (−/−) mice die without showing signs of DNA fragmentation.

Because ERK inhibition efficiently prevented PM damage and nuclear condensation, but had only a delaying effect on DNA damage (Table I), we investigated if ERK activation regulates caspase-3 cleavage (activation), which is known to orchestrates DNA damage (Enari et al., 1998). Caspase-3 is activated in parallel to pERK after potassium deprivation (Fig. 4 B). Both PD98059 (50 μM) and U0126 (20 μM) failed to prevent cleavage of the active caspase-3 subunit, and they did not affect its activity (Fig. 4, C and E), suggesting that inhibition of ERK does not prevent caspase-3 cleavage nor caspase-3 activity. Because treatment with U0126 somewhat delayed DNA damage (Table I), it is conceivable that ERK may act on downstream targets of caspase-3 to promote DNA fragmentation. MEK/ERK inhibitors prevented ERK activation, implying their activity in these treatments, with U0126 being more potent than PD98059 (Fig. 4 C).

Effect of the pan caspase inhibitor on neuronal degeneration

In addition to preventing PM damage, inhibition of ERK also prevented nuclear condensation independent of caspase-3. >14 mammalian caspases have been identified so far (Chinnaiyan and Dixit, 1996). Therefore, it is conceivable that ERK may induce cell demise through any of these cas-

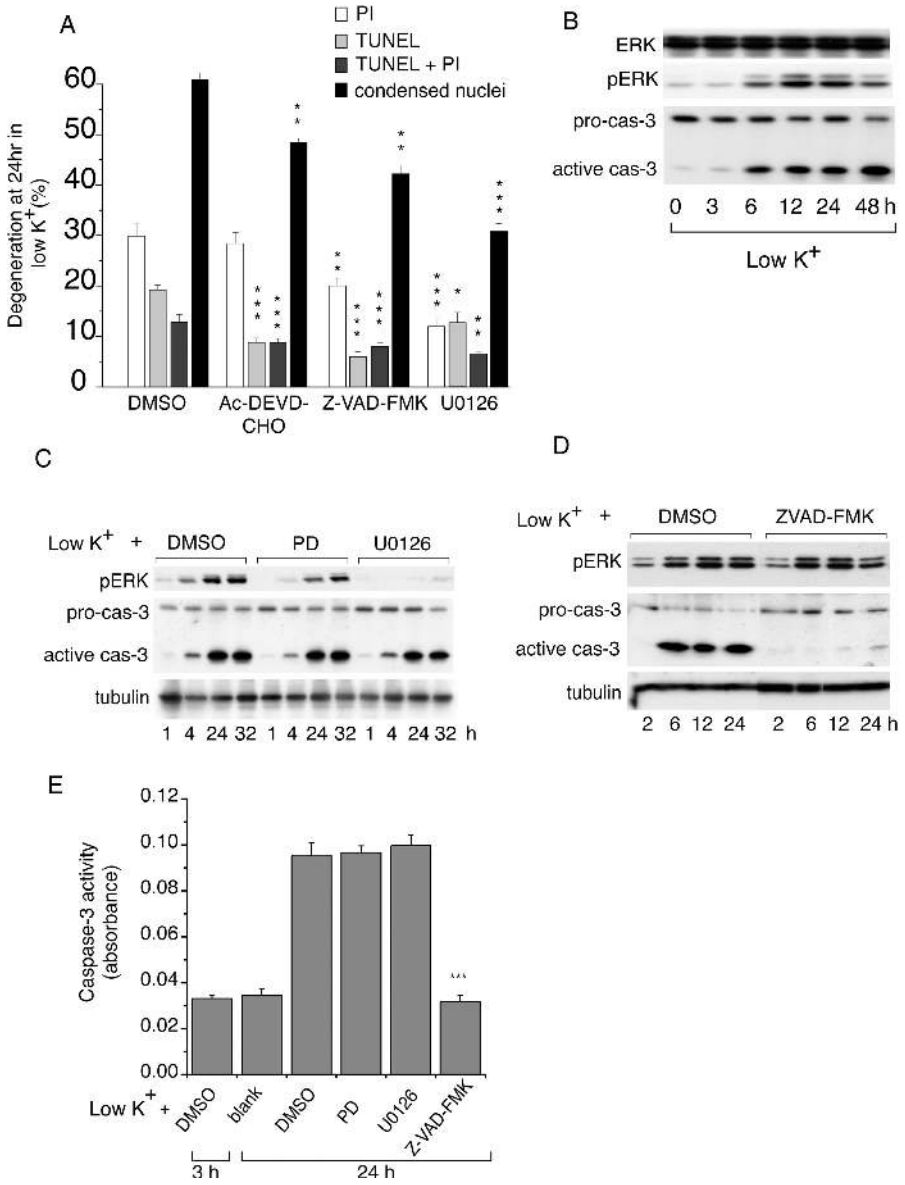

Figure 4. **The role of caspase in CGN degeneration.** (A) Caspase-3 and pan caspase inhibitors selectively prevent neuronal degeneration. After potassium change (low K^+), neurons were incubated with 0.5% DMSO, 100 μM caspase-3 inhibitor Ac-VAD-CHO, 100 μM pan caspase inhibitor Z-VAD-FMK, or 20 μM U0126 for 24 h, and triple staining was performed. Data represent the total number of neurons positive for PI (PM damaged), TUNEL (DNA damaged), TUNEL + PI (both DNA and PM damaged), and neurons with CN. ***$P < 0.001$, **$P < 0.01$, and *$P < 0.05$ was compared with DMSO treatment. (B) Caspase-3 is activated (active cas-3) in parallel to ERK activation. Cells were harvested at the indicated time points and processed for Western blot analysis to detect total ERK (ERK), pERK, and caspase-3 (pro and active fragment). (C) MEK/ERK inhibitors do not prevent caspase-3 cleavage. Cells were harvested after 50 μM PD98059 or 20 μM U0126 treatment and probed for pERK, caspase-3, and tubulin. (D) Pan caspase inhibitor blocks caspase-3 activation but shows no effect on ERK activation. Cells were harvested after 100 μM Z-VAD-FMK or 0.2% DMSO treatment, and Western blot analysis was performed for pERK, caspase-3, and tubulin. (E) Measurement of caspase-3 activity. 50 μM PD98059, 20 μM U0126, 100 μM Z-VAD-FMK, or 0.2% DMSO was added for the indicated time points, and cell extracts were assayed for caspase-3 activation. The control assay was performed without the cell extract (blank).

pases. To test this possibility, we made use of the pan caspase inhibitor benzyloxycarbonyl-Val-Ala-Asp-fluoromethylketone (Z-VAD-FMK). Treatment with Z-VAD-FMK (100 μM) significantly reduced both PM damage and nuclear condensation compared with the specific caspase-3 inhibitor. However, neither of the two (pan caspase or caspase-3 specific inhibitor) was as effective as the ERK inhibitor U0126 in preventing PM damage and nuclear condensation (Fig. 4 A). Together, these data suggest that both ERK and caspases other than caspase-3 are involved in promoting neuronal degeneration. In addition, Z-VAD-FMK attenuated both caspase-3 cleavage and its activity, but failed to prevent ERK activation, suggesting that ERK is either upstream or independent of caspases in this paradigm (Fig. 4, D and E).

ERK translocates to the nucleus and caspase-3 remains in the cytoplasm

Activation of ERK1/2 results in its translocation from the cytoplasm to the nucleus, where it phosphorylates and regulates the activity of several transcription factors (Reiser et al., 1999). To test if pERK translocates to the nucleus in CGN, we performed PI/DAPI or TUNEL/DAPI staining followed by the immunocytochemical visualization of pERK. After the 6 h of potassium switch, the majority (~58%) of the neurons displayed pERK immunoreactivity in the cytoplasm (Fig. 5 A, arrowheads; and Fig. 5 B) compared with its nuclear localization (~8%). In contrast, 42% of the neurons at 24 h displayed high pERK immunoreactivity in the nucleus (Fig. 5 A, arrows and asterisks; and Fig. 5 B), and ~28% of the neurons showed pERK staining still in the cytoplasm (Fig. 5 B). These data suggest that ERK is activated in the cytoplasm as early as 6 h and undergoes nuclear translocation to regulate genes or proteins required for promoting neuronal degeneration.

The quantification of pERK immunoreactivity in PM- and DNA-damaged neurons is shown in Fig. 5 C. At 24 h, a majority of PM-damaged neurons (~45%) are positive for nuclear translocated pERK (nuclear pERK/PI+) compared with DNA-damaged neurons (~12%, nuclear pERK/TUNEL+).

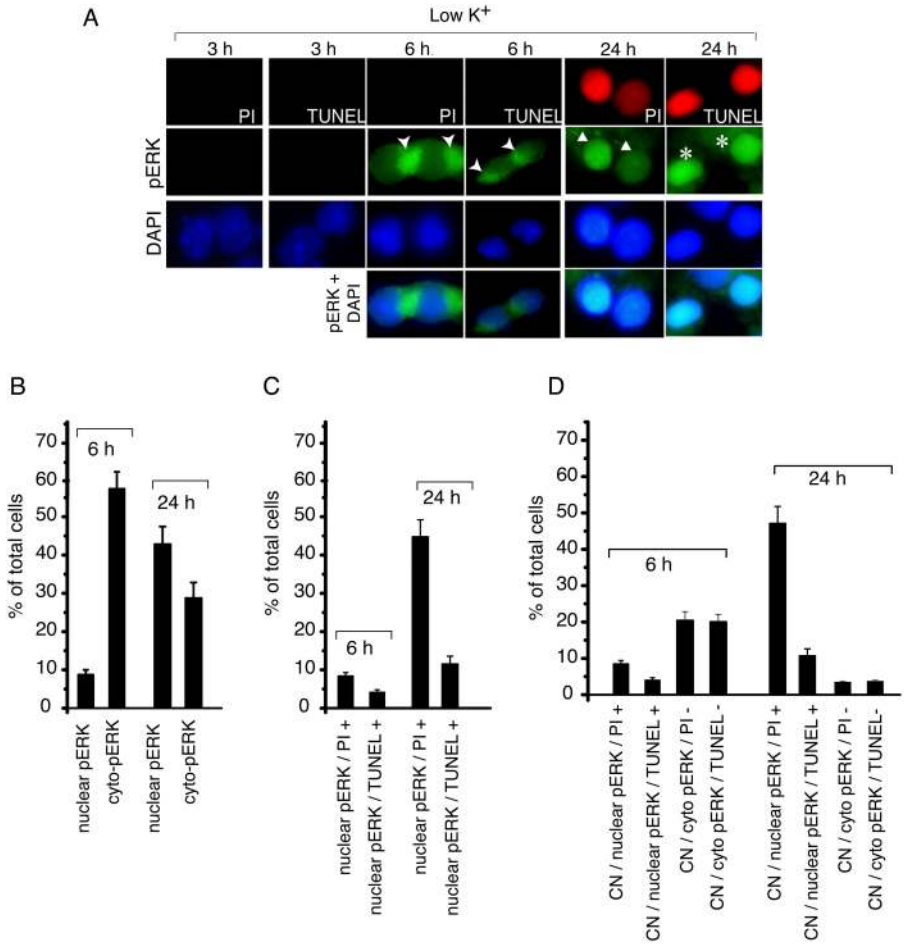

Figure 5. **Cellular distribution of pERK in subsets of damaged neurons.** (A) Fluorescence microscopy of the pERK in damaged neurons. After potassium change (low K^+), CGN were processed for pERK immunocytochemistry combined with either TUNEL or PI staining and nuclear staining (DAPI) for 3, 6, and 24 h. arrowheads, pERK in the cytoplasm and corresponding TUNEL or PI-negative neurons; arrows, pERK in the nucleus and corresponding PI- stained neurons; asterisks, pERK in the nucleus and corresponding TUNEL-positive neurons. (B) Quantification of the cellular distribution of pERK at 6 and 24 h after potassium change, in the nucleus (nuclear pERK), and in the cytoplasm (cyto pERK). (C) Quantification of pERK in damaged neurons at 6 and 24 h. (D) Quantification of pERK immunoreactivity in CN with cellular damage at 6 and 24 h. Error bars represent mean ± SEM from at least three experiments.

This finding suggests that the same percentage of cells that shows pERK nuclear immunoreactivity eventually undergoes PM damage (Fig. 5, compare B and C). In addition, a larger number of nuclear pERK/PI+ neurons compared with nuclear pERK/TUNEL+ neurons further corroborate the finding that ERK activation predominantly directs PM damage (Fig. 5 C and Table I). It should be noted that the large number of PI-positive neurons are nuclear pERK positive (~45%) compared with only PI–positive neurons (Table I, ~31%). These 45% of the PI-positive neurons with nuclear pERK are the combined total of all PI positive neurons (Table I, only PI [31%] plus TUNEL + PI [13%]).

At 6 h in low potassium, ~20% of the neurons with cytoplasmic pERK immunoreactivity (Fig. 5 A, arrowheads) were neither PI nor TUNEL positive (Fig. 5 D) but had already undergone changes in their nuclear morphology associated with prominent condensation (evident in DAPI staining). These observations indicate that an intense ERK activation occurs in the cytoplasm, and that changes in nuclear morphology occur before PM or DNA damage (Table II, 6 h).

Next, we analyzed the cellular localization of caspase-3 and its distribution in different subsets of damaged neurons. Activated caspase-3 remains restricted to the cytoplasm of neurons (Fig. 6 A; and Fig. 6 D, arrows). A larger number of DNA-damaged neurons appeared positive for caspase-3 (cyto-cas-3/TUNEL+) compared with PM-damaged (cyto-cas-3/PI+) neurons (Fig. 6 B), indicating that caspase-3 activation is predominantly associated with DNA damage in CGN. Fig. 6 C shows that PI-positive neurons (PM damage, arrow) are negative for caspase-3. In contrast, TUNEL-positive neurons (DNA damage; Fig. 6 C, asterisks) are positive for caspase-3, further corroborating the finding that PM damage in CGN is not associated with caspase-3 activation. Colocalization of pERK and caspase-3 revealed that at 24 h after potassium withdrawal ~15% of the neurons were double-stained for pERK and caspase-3 (Fig. 6, D and E). Note that caspase-3 remained in the cytoplasm (Fig. 6 D, arrow) and pERK translocated to the nucleus (Fig. 6 D, arrowhead) at 24 h in low K^+.

Effect of antioxidants and protein synthesis inhibitor in neuronal damage

We tested the effect of antioxidants on cellular damage. Both the antioxidant N-acetyl cystein (N-AC; 5 mM) and superoxide dismutase (SOD; 50 U/ml) significantly reduced numbers of neurons with CN and PM damage but failed to prevent DNA damage (Fig. 7 A). Previous works have shown that ROS can activate ERK. Therefore, we investigated the effect of N-AC and SOD on ERK as well as caspase-3 activation. Both N-AC and SOD reduced ERK activation for the time points analyzed (6 and 12 h), but failed to prevent caspase-3 cleavage as well as its activity (Fig. 7 B).

Next, the effect of the protein synthesis inhibitor cyclohexamide (CHX) on nuclear condensation, PM and DNA

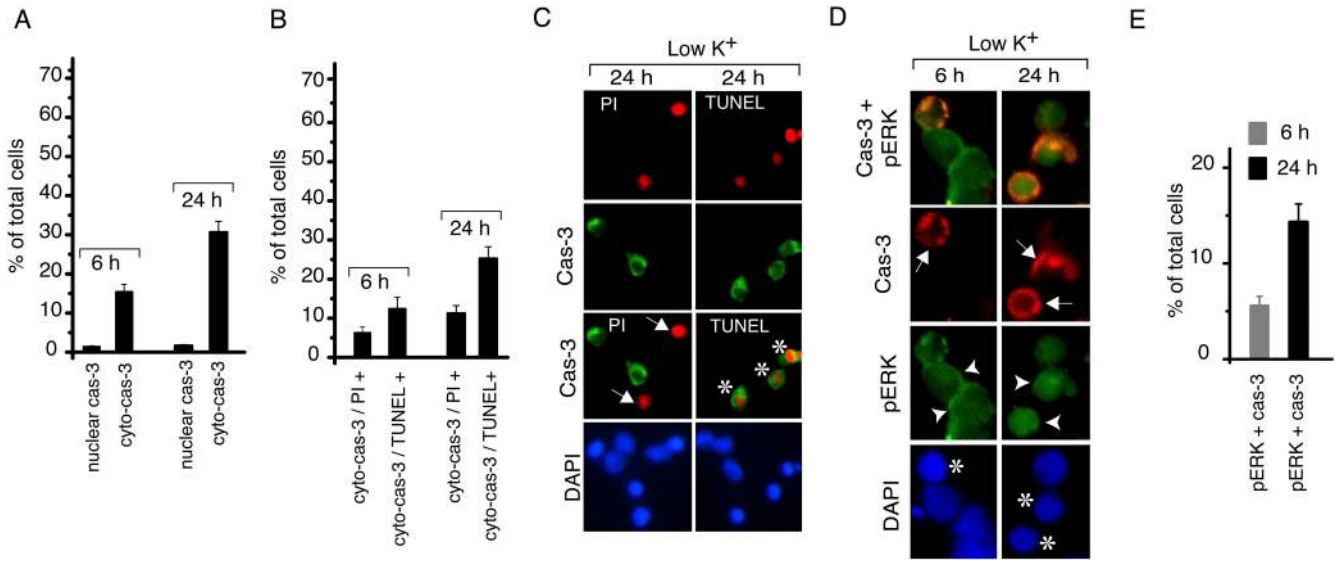

Figure 6. **Cellular distribution of activated caspase-3 in subsets of damaged neurons.** After potassium change (low K^+), CGN were processed for immunocytochemical detection of cleaved (activated) caspase-3 combined with either TUNEL or PI staining and nuclear staining (DAPI) for 6 and 24 h. (A) Quantification of the cellular distribution of caspase-3 at 6 and 24 h after potassium change in the nucleus (nuclear cas-3) and in the cytoplasm (cyto cas-3). (B) Quantification of caspase-3 immunoreactivity in damaged neurons at 6 and 24 h. (C) Fluorescence microscopy immunodetection of caspase-3 in damaged neurons at 24 h. PM-damaged (PI) neurons are negative for caspase-3 (arrows), and DNA damaged (TUNEL) neurons are positive for caspase-3 (asterisks). (D) Colocalization of pERK and caspase-3 after potassium change at 6 and 24 h. Arrows, caspase-3–positive cells; arrowheads, pERK-positive cells; asterisks, CN. (E) Quantification of pERK and caspase-3 colocalization. Error bars represent mean ± SEM from at least three experiments.

damage was investigated. CHX treatment (10 μg/ml) dramatically diminished all cellular damage (Fig. 7 A). To further unravel signaling mechanisms, by which CHX prevented cellular damage, we determined levels of pERK and caspase-3 in CGN cultures treated with CHX. CHX treatment abrogated both ERK activation and caspase-3 activity, indicating the requirement of new proteins for ERK and caspase-3 activation (Fig. 7, B and C).

Next, we tested the possibility that CHX may act directly by binding to ERK and caspase-3 rather than inhibiting the synthesis of protein. CHX added at 0 and 12 h and cell lysates were processed to detect pERK and caspase-3 at 13 h after the potassium change. CHX added at 0 h effectively abolished caspase-3 and ERK activation but did not do so at 12 h, suggesting that CHX specifically acts by inhibiting protein synthesis (Fig. 7 D). If CHX can act directly, by binding to ERK and caspase-3, it should have done so even when added at 12 h, as U0126, which effectively abrogated ERK activation when added even at 12 h. U0126 directly binds to MEK and thereby attenuates ERK activation (Favata et al., 1998). Note that U0126 failed to inhibit caspase-3 cleavage (Fig. 7 D).

Together, these results indicate that the "death" phenotypes of CGN after potassium withdrawal are heterogeneous, allowing to distinguish between PM-, DNA-, and membrane/DNA-damaged populations. Most of these damaged neurons display nuclear condensation, which is an early event that precedes PM or DNA damage. As summarized in Fig. 8, we have demonstrated by using various inhibitor strategies that ERK inhibition results in a dramatic reduction of PM-damaged neurons and nuclear condensation, underscoring the crucial role played by ERK in CGN degeneration. Interestingly, this effect of ERK is independent of caspase-3. In contrast, inhibition of caspase-3 largely prevented DNA damage and moderately reduced nuclear condensation (Fig. 8, open arrow) without affecting PM damage. The dotted arrow indicates late PM damage in DNA-damaged neurons (Fig. 8).

Discussion

Low potassium triggers a unique mode of cell death

The present work shows that degeneration of CGNs induced by switching from high to low potassium occurs along three distinct routes toward death: (1) cells undergoing only PM damage, (2) cells that exhibit only DNA damage, and (3) cells exhibiting both DNA and PM damage. Most neurons showing either or both of these cellular phenotypes also have CN. CGN death following potassium deprivation has been considered to be apoptotic (D'Mello et al., 1993; Miller and Johnson, 1996). Condensation of nuclei and DNA fragmentation are widely accepted as essential features of cells undergoing apoptosis (Vaux, 1993; Majno and Joris, 1995). If at all, PM damage has been conceived as a late event in apoptosis (Vaux, 1993). Neurons with exclusive DNA damage or a combination of DNA and PM damage (thought to represent a late stage of apoptosis) fulfill salient criteria of apoptosis. The large population of CGN showing PM damage only contradicts the hypothesis that CGN cell death occurs exclusively by apoptosis. Cell swelling, with an early loss of PM integrity and major changes of organelles, including nuclear swelling, are considered as essential features of cells undergoing necrosis (Vaux, 1993). Thus, those CGN exhibiting signs

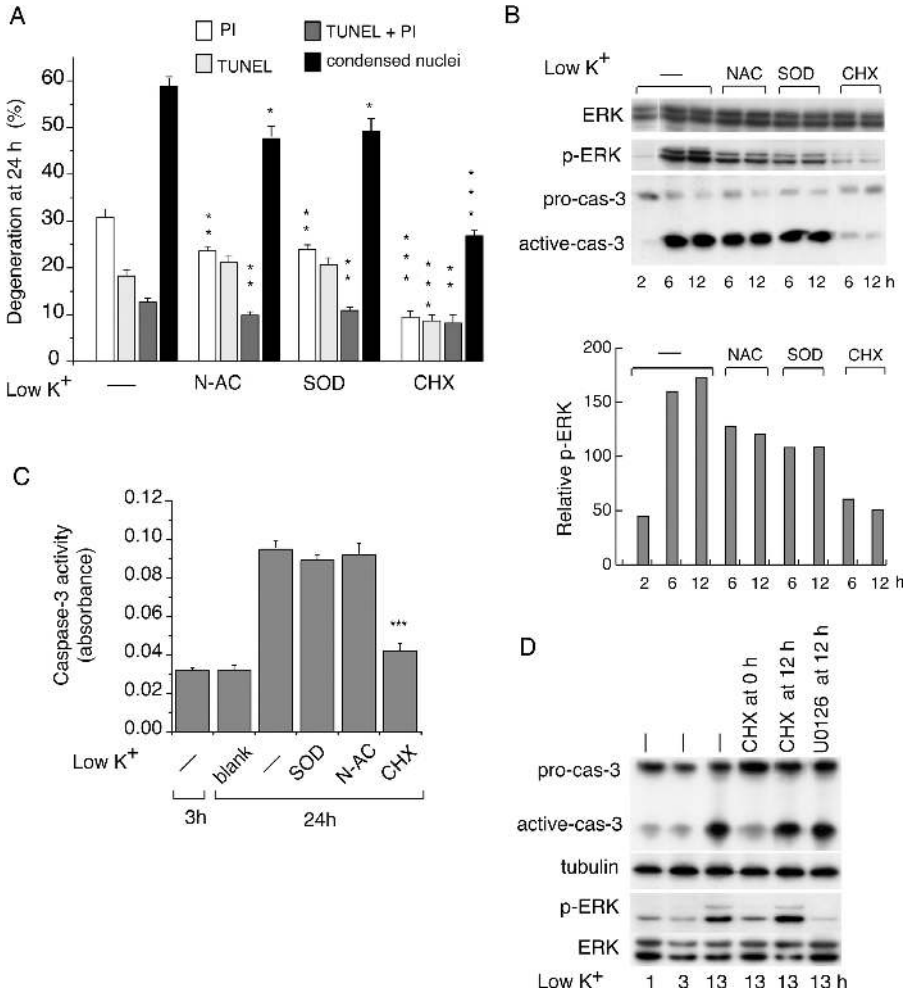

Figure 7. **Effect of antioxidants and protein synthesis inhibitor on neuronal degeneration and ERK/caspase-3 activation.** At the time of potassium change (low K^+), 5 mM N-acetyl cysteine (N-AC), 50 U/ml superoxide dismutase (SOD), or 10 g/ml cyclohexamide (CHX) was added; and triple staining and Western blot analysis were performed at the indicated time points. (A) The triple staining for the aforementioned groups at 24 h. ***$P < 0.001$, **$P < 0.01$, and *$P < 0.05$ compared with untreated cultures. (B) Western blot probed for total ERK (ERK), p-ERK, and caspase-3. (C) 5 mM N-AC, 50 U/ml SOD, and 10 g/ml CHX were added immediately after potassium change, and cell extracts were assayed for caspase-3 activation; —, untreated; blank, without cell extract. Error bars represent mean ± SEM from at least six experiments. (D) CHX does not act by binding to ERK and caspase-3. 10 g/ml CHX was added at 0 and 12 h after the potassium switch. 20 μM U0126 was added at 12 h. The cell lysates were isolated after 13 h and processed for caspase-3 and ERK activation. Tubulin and total ERK blots reveal total protein loading.

of PM damage at relatively early stages after potassium withdrawal may be conceived to undergo necrosis. However, these neurons showed significant condensation rather than swelling of nuclei. Therefore, the absence of DNA fragmentation and the occurrence of necrotic-like PM damage with apoptotic-like nuclear condensation suggest that low potassium induces an unusual type of cell death, which does not meet the criteria of classical necrosis or classical apoptosis, respectively.

There is a growing debate regarding the definition of distinct categories of cell death. For example, a clear-cut distinction between apoptosis and necrosis is getting increasingly difficult because both modes of cell death share common features. Over the last years, exceptions have been found for essentially all of the criteria that define apoptosis (Maher and Schubert, 2000; Kanduc et al., 2002; Sloviter, 2002). Using an established model of neuronal cell death, our data reveal that the cell death "phenotypes" are not only heterogeneous but also display features of yet undefined forms of cell death. At present, it is unclear how to categorize neurons with only PM damage. The occurrence of cell death that fulfills neither the criteria of apoptosis nor necrosis has been documented in various cell types including neurons (Pilar and Landmesser, 1976; Clarke, 1990; Cornillon et al., 1994; Dal Canto and Gurney, 1994; Jurgensmeier et al., 1997). Particularly interesting is the IGF1R-induced cell death of 293T cells called "paraptosis" that shares some of the features described in our paper (Sperandio et al., 2000). Thus, paraptosis includes relative resistance to caspase inhibitors, absence of TUNEL staining, chromatin condensation, and cyclohexamide dependence. However, cytoplasmic vacuolation, an essential characteristic feature of paraptosis, was not observed in our EM analyses of low potassium-induced cell death (unpublished data). This suggests that paraptosis and CGN neuron death may be two different entities.

ERK promotes PM damage

Although a role of ERK activation in cell death has been suggested for other neuronal systems (Alessandrini et al., 1999; Stanciu et al., 2000), the underlying mechanisms and intracellular networks linking ERK activation to the specific cellular damage were previously unknown. We have now shown for the first time a role of ERK activation in promoting exclusively PM damage independent from caspase-3–mediated apoptotic cell death. Inhibition of ERK not only reduced the percentage of the PM-damaged subpopulation of neurons but also decreased the late PM damage in neurons with DNA damage. This finding suggests that ERK activation is indispensable for PM damage. In contrast to the prominent effect of ERK inhibition on PM damage, its effect on DNA damage was only transient (at 12 and 24 h). In

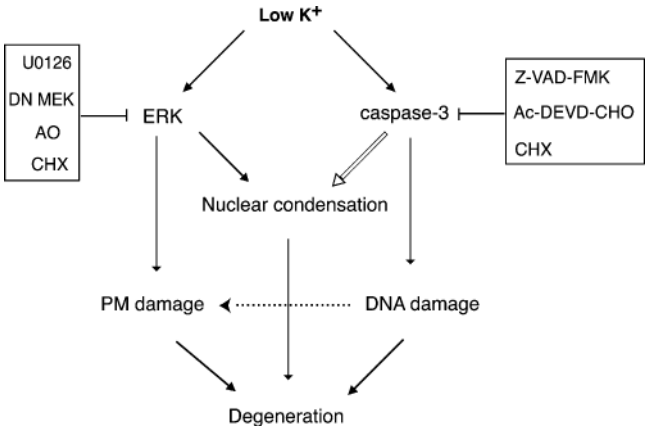

Figure 8. **Diagram summarizing the role of ERK and caspase-3 in the degeneration of CGN.** U0126, MEK1/2 inhibitor; Z-VAD-FMK, pan caspase inhibitor; Ac-DEVD-CHO, caspase-3 inhibitor; AO, antioxidants; CHX, cyclohexamide. For description, see the end of the Results section.

addition, ERK inhibition also provided significant protection on nuclear condensation, thus expanding its role not only as an executer of PM damage but also of nuclear condensation (Table I). It should be noted that CA-MEK does not induce apparent cell death in high potassium culture (Fig. 3 E). We and others (Miller et al., 1997b) have observed that high potassium CGN culture exhibit an elevated ERK activation, and an abolishment of ERK activation by MEK inhibitors does not interfere with the high potassium-mediated CGN survival (unpublished data). This observation suggests that the high potassium-promoted survival is independent of ERK activation. Therefore, overexpression of CA MEK had no apparent effect on CGN survival in high potassium.

Caspase-3 is not required for PM damage

Further, we analyzed the localization of activated ERK (pERK) in an attempt to understand the expression pattern of pERK in these damaged neurons. Interestingly, an intense nuclear localization of pERK immunoreactivity was observed in both PI-stained and TUNEL-stained neurons, however, with different proportions. A large number of PM-damaged neurons were pERK positive compared with DNA-damaged neurons at 24 h. This result further suggests that ERK activation is predominantly involved in PM damage. Even though ERK activation could be observed in DNA-damaged neurons, the failure of ERK inhibition (upon U0126 treatment) to afford strong protection against DNA damage hints to the possibility of an involvement of an ERK-independent pathway to promote DNA damage.

One such potential pathway is the caspase-3–dependent pathway. Several lines of evidence suggest that caspase-3 crucially controls cellular changes related to apoptosis (Chinnaiyan and Dixit, 1996). In our paradigm blocking of caspase-3 largely prevented DNA, but not PM, damage. In addition, our immunofluorescense study of caspase-3 and pERK in subsets of damaged neurons suggests that DNA and PM damage are controlled by distinct molecular mechanisms: pERK promotes PM damage, and caspase-3 promotes DNA damage. Furthermore, a pan caspase inhibitor, which attenuated caspase-3 activation but failed to prevent ERK activation, corroborates the notion that caspase-3 and ERK not only command distinct cellular damage but also act independently in the process of neuronal degeneration.

Interestingly, ERK is activated in the cytoplasm, but showed a prominent nuclear localization in neurons with CN. Similarly, active caspase-3 was also seen in the cytoplasm of neurons, but only in those with CN (Fig. 6 D). The fact that ERK promotes cell death independent of caspase-3, together with this differential expression pattern, suggests that ERK and caspase-3 may use distinct targets to advance the process of neuronal degeneration. Although ERK seems to modulate both cytoplasmic and nuclear targets, caspase-3 may rather focus on cytoplasmic substrates.

A model for the two distinct pathways involving ERK and caspase-3 activation for the performance of two distinct types of cell damage is presented in Fig. 8. It is not clear as yet whether or not ERK acts independently of all known caspases. The fact that a general caspase inhibitor was more potent in preventing neuronal degeneration than the specific caspase-3 inhibitor suggests that ERK may target caspases other than caspase-3 for promoting degeneration. Nevertheless, the more robust protection by inhibiting ERK rather than caspases (Fig. 4 A) suggests that ERK activation plays a major role in CGN death after potassium deprivation, possibly independent of all known caspases.

A caspase-independent mechanism of cell death has been reported in various other models of neuronal cell death. Cell death induced by methyl mercury in CGN (Castoldi et al., 2000), by serum deprivation in cortical neurons (Hamabe et al., 2000), by kainic acid in CGN (Verdaguer et al., 2002), and by H_2O_2 in PC12 cells (Jiang et al., 2001) has been reported to be independent of caspases. In addition, it has been proposed that loss of CGN viability maintained in low potassium might involve a mechanism independent of caspases (Miller et al., 1997a). As our study demonstrates for the first time, ERK acts independently of caspase-3 to promote degeneration in this paradigm, it is tempting to speculate that the ERK pathway may be part of a largely caspase-independent mechanism of neuronal cell death.

Potential targets and regulators of ERK

We have previously shown that one of the potential targets of ERK activation is c-Jun protein expression and phosphorylation (Subramaniam et al., 2003), a prerequisite for CGN death (Watson et al., 1998). Interestingly, the early growth response gene-1 (Egr-1) is activated at 6 h (i.e., at the time when ERK is also activated) and induces c-Jun activation, which promotes cell death in this paradigm (Levkovitz and Baraban, 2002). *egr-1* contains five serum response elements and can be regulated by Elk1, a key component binding to serum response elements (Cibelli et al., 2002). It has been demonstrated that Elk-1 is a target of ERK (Davis, 1993). Because Elk-1 controls *egr-1*, which in turn controls c-Jun activation (Levkovitz and Baraban, 2002), we hypothesize that ERK may indirectly activate c-Jun via the intermediate targets Elk-1 and

Egr-1. In addition, it has been demonstrated that ERK directly phosphorylates c-Jun (Pulverer et al., 1991), raising the possibility that ERK is directly involved in the regulation of c-Jun.

We have previously demonstrated that ROS acts upstream of ERK in this CGN paradigm (Subramaniam et al., 2003). The use of two different antioxidants (N-AC and SOD) prevented ERK activation only in part (~40%), suggesting that ROS acts upstream of ERK but contributes partially to ERK activation. Interestingly (Noshita et al., 2002), it has been demonstrated that overexpression of SOD1 prevents cell death after transient focal cerebral ischemia by preventing ERK1/2 activation, suggesting that ROS acts upstream of ERK.

Growing evidence suggests that ERK activation is prominently involved in neurodegeneration, including animal models of ischemia (Alessandrini et al., 1999; Noshita et al., 2002). With regard to human neurodegenerative disorders, phosphorylated ERK immunoreactivity has been found in neurons in Pick's disease, progressive supranuclear palsy, and corticobasal degeneration (Ferrer et al., 2001). In Alzheimer's disease, phosphorylated ERK immunoreactivity in a granular appearance has been described in a subpopulation of hippocampal neurons with neurofibrillar degeneration (Perry et al., 1999). More recently, granular cytoplasmic aggregates of pERK have been shown in the substantia nigra of patients with Lewy body disease (Zhu et al., 2002), suggesting a possible role of ERK activation in this human neurodegenerative disorder.

In summary, the present work provides evidence not only for the generation of different morphological phenotypes of damaged neurons but also for the unique role of ERK in the execution of PM damage through a mechanism that is independent of caspase-3. It remains to be resolved whether or not this mechanism operates also in other neuronal death paradigms.

Materials and methods

Cell culture

CGN were isolated and cultured from 8-d-old Wistar rats as described previously (Subramaniam et al., 2003). Cells were resuspended in high K^+ (Eagle's basal medium containing 10% FCS, 25 mM KCl, 2 mM glutamine, and 0.5% [vol/vol] penicillin/streptomycin), switched to low K^+ (Eagle's basal medium, 5 mM KCl, 2 mM glutamine, and 0.5% penicillin/streptomycin) at day 4, treated with additives for the indicated time points, and processed for the specific assays described in the following paragraph.

Triple staining for PI uptake, TUNEL, and DAPI

At the indicated time points, 5 μg/ml PI, an established marker for PM damage, was added directly to the culture medium and incubated at 37°C for 10 min. Cells were washed and fixed with 4% PFA, permeabilized with 0.2% Triton X-100, and processed for TUNEL (Promega). 5 μg/ml DAPI was added to stain cell nuclei. Photomicrographs from 4–6 different fields in each coverslip were captured under red (PI), green (TUNEL), and blue (DAPI) channels and merged using adobe photoshop 5.5. Typically, ~500 cells were analyzed for the number of only PI-stained (PM damaged) or only TUNEL-positive (DNA damaged), or both TUNEL- and PI-positive (DNA and PM damaged) neurons. Total numbers of neurons with CN were also counted wherever indicated. Cell numbers were presented as a percentage of degenerated cells in relation to total cell numbers.

Acquisition of microscope images

Cells were examined with a computer-controlled fluorescence microscope (model Axioplan 2 imaging; Carl Zeiss MicroImaging, Inc.) equipped with a high resolution digital camera (model Axiocam; Carl Zeiss MicroImaging, Inc.) under control of Axiovision 3.1 software (Carl Zeiss MicroImaging, Inc.). Depending on the experiments, images were made using 20, 40, or 63× Neofluar objectives with numerical aperture 0.5, 0.75, and 1.25, respectively.

Preparation and infection of recombinant adenoviruses

CA-MEK-1, cDNAs (G1C, ΔN4-S218E/S222D) encoding an HA epitope tag, was provided by N. Ahn (University of Toronto, Toronto, Ontario, Canada; Mansour et al., 1996). HA-tagged K97M DN mutant form of MEK, CA MEK, and GFP were cloned and expressed in adenoviruses as described previously (Mazzoni et al., 1999; Shalin et al., 2004). Recombinant adenoviruses expressing GFP were used to determine MOI. Infection rates 55% to 80% were routinely obtained with 300–500 MOI. 350 MOI was used for all the experiments. On DIV2.5, CGN were infected with adenoviruses expressing DN MEK, CA MEK, or GFP, and on DIV4, medium was changed to low potassium. On DIV5, cells were processed for cell death and Western blot analysis. Cell death was presented as a percentage of total cells that were PM damaged or exhibited CN. Western blot analysis was performed to detect overexpressed HA-MEK using an antibody against MEK1/2 (New England Biolabs, Inc.).

Quantification of pERK and caspase-3 localization in damaged neurons

After the potassium switch, the cells were processed for the following combinations of staining: pERK/PI/DAPI, pERK/TUNEL/DAPI, caspase-3/PI/DAPI, and caspase-3/TUNEL/DAPI, for the indicated time points. The percentages of pERK- or caspase-3–positive cells were determined by counting 500 cells per field. Cell numbers were presented as percentages of stained cells in each subset (PI positive and TUNEL positive) in relation to the total cell number.

Nuclear size measurements

The area of DAPI-stained nuclei of normal (neither PI nor TUNEL stained), only PI-stained, only TUNEL-stained, or both TUNEL and PI-stained neurons were measured using Image tool 3.0 software (UTHSCSA).

Immunocytochemistry

Cells were fixed in 4% PFA, permeabilized with 0.2% Triton X-100, and blocked with 5% normal horse serum followed by incubation with an mAb for pERK or a polyclonal antibody for cleaved caspase-3. Cells were incubated with anti–mouse IgG conjugated with CY2. In the case of pERK or caspase-3/PI costaining, PI was added before fixing the cells. In the case of pERK or caspase-3/TUNEL costaining, TUNEL staining was performed before pERK or caspase-3 immunocytochemistry as aforementioned using streptavidin CY3. In the case of the pERK/caspase-3 visualization, the antibody against pERK was incubated overnight followed by incubation with the antibody for cleaved caspase-3. Cultures were incubated with CY2-conjugated anti–mouse and CY3-conjugated anti–rabbit antibody, respectively. 5 μg/ml DAPI was added in all cases. Immunostaining for overexpressed DN MEK and CA MEK was performed using polyclonal antibody against HA-tagged epitope (Babco).

All other antibodies were obtained from New England Biolabs, Inc. All CY2/CY3-conjugated fluoroprobes were obtained from Dianova.

Western blot analysis

Western blot analysis was performed exactly as described previously (Subramaniam et al., 2003).

Assay of caspase-3 enzymatic activity

Caspase-3 activity was assayed as described previously (Verdaguer et al., 2002). Results were expressed as units of absorbance. Caspase-3 inhibitors Ac-DEVD.CHO, Z-VAD-FMK, U0126, and PD98059 were obtained from Promega.

Statistical analysis

Data were expressed as means ± SEM. All experiments were performed in triplicates or duplicates and repeated at least three times. Statistical analysis among groups was performed using *t* test (Origin 6.1). P-values are as follows: */°$P < 0.05$, **/°° $P < 0.01$, and ***/°°°$P < 0.001$.

Online supplemental material

Fig. S1 indicates the role of JNK and p38 in inducing PM or DNA damage. Low potassium-containing CGN culture exhibits high JNK and low p38 activation. p38 inhibitor SB203580 has no apparent effect on PM or DNA damage. JNK inhibitor, JNKI1, provides a small but significant protection on PM

damage, through a yet unknown mechanism. Online supplemental material is available at http://www.jcb.org/cgi/content/full/jcb.200403028/DC1.

We thank Jutta Fey, Marion Schmitt, Gerald Bender, and Barbara Brühl for technical assistance and Dr. Neelam Shahani for critically reading the manuscript.

This work was supported by the Deutsche Forschungsgemeinschaft (STR 616/1-2), SFB 488, and a fellowship to S. Subramaniam from Graduiertenkolleg 791, University of Heidelberg, Germany. This work was also supported by fellowships and grants to U. Zirrgiebel and D. Kaplan from the National Cancer Institute of Canada and the Canadian Institutes for Health Research.

Submitted: 3 March 2004
Accepted: 21 March 2004

References

Alessandrini, A., S. Namura, M.A. Moskowitz, and J.V. Bonventre. 1999. MEK1 protein kinase inhibition protects against damage resulting from focal cerebral ischemia. *Proc. Natl. Acad. Sci. USA.* 96:12866–12869.

Bhat, N.R., and P. Zhang. 1999. Hydrogen peroxide activation of multiple mitogen-activated protein kinases in an oligodendrocyte cell line: role of extracellular signal-regulated kinase in hydrogen peroxide-induced cell death. *J. Neurochem.* 72:112–119.

Castoldi, A.F., S. Barni, I. Turin, C. Gandini, and L. Manzo. 2000. Early acute necrosis, delayed apoptosis and cytoskeletal breakdown in cultured cerebellar granule neurons exposed to methylmercury. *J. Neurosci. Res.* 59:775–787.

Chinnaiyan, A.M., and V.M. Dixit. 1996. The cell-death machine. *Curr. Biol.* 6:555–562.

Cibelli, G., V. Policastro, O.G. Rossler, and G. Thiel. 2002. Nitric oxide-induced programmed cell death in human neuroblastoma cells is accompanied by the synthesis of Egr-1, a zinc finger transcription factor. *J. Neurosci. Res.* 67: 450–460.

Clarke, P.G. 1990. Developmental cell death: morphological diversity and multiple mechanisms. *Anat. Embryol. (Berl.).* 181:195–213.

Cornillon, S., C. Foa, J. Davoust, N. Buonavista, J.D. Gross, and P. Golstein. 1994. Programmed cell death in *Dictyostelium*. *J. Cell Sci.* 107:2691–2704.

D'Mello, S.R., C. Galli, T. Ciotti, and P. Calissano. 1993. Induction of apoptosis in cerebellar granule neurons by low potassium: inhibition of death by insulin-like growth factor I and cAMP. *Proc. Natl. Acad. Sci. USA.* 90:10989–10993.

D'Mello, S.R., C.Y. Kuan, R.A. Flavell, and P. Rakic. 2000. Caspase-3 is required for apoptosis-associated DNA fragmentation but not for cell death in neurons deprived of potassium. *J. Neurosci. Res.* 59:24–31.

Dal Canto, M.C., and M.E. Gurney. 1994. Development of central nervous system pathology in a murine transgenic model of human amyotrophic lateral sclerosis. *Am. J. Pathol.* 145:1271–1279.

Davis, R.J. 1993. The mitogen-activated protein kinase signal transduction pathway. *J. Biol. Chem.* 268:14553–14556.

Enari, M., H. Sakahira, H. Yokoyama, K. Okawa, A. Iwamatsu, and S. Nagata. 1998. A caspase-activated DNase that degrades DNA during apoptosis, and its inhibitor ICAD. *Nature.* 391:43–50.

Favata, M.F., K.Y. Horiuchi, E.J. Manos, A.J. Daulerio, D.A. Stradley, W.S. Feeser, D.E. Van Dyk, W.J. Pitts, R.A. Earl, F. Hobbs, et al. 1998. Identification of a novel inhibitor of mitogen-activated protein kinase kinase. *J. Biol. Chem.* 273:18623–18632.

Ferrer, I., R. Blanco, M. Carmona, R. Ribera, E. Goutan, B. Puig, M.J. Rey, A. Cardozo, F. Vinals, and T. Ribalta. 2001. Phosphorylated map kinase (ERK1, ERK2) expression is associated with early tau deposition in neurones and glial cells, but not with increased nuclear DNA vulnerability and cell death, in Alzheimer disease, Pick's disease, progressive supranuclear palsy and corticobasal degeneration. *Brain Pathol.* 11:144–158.

Guyton, K.Z., Y. Liu, M. Gorospe, Q. Xu, and N.J. Holbrook. 1996. Activation of mitogen-activated protein kinase by H_2O_2. Role in cell survival following oxidant injury. *J. Biol. Chem.* 271:4138–4142.

Hamabe, W., N. Fukushima, A. Yoshida, and H. Ueda. 2000. Serum-free induced neuronal apoptosis-like cell death is independent of caspase activity. *Brain Res. Mol. Brain Res.* 78:186–191.

Hengartner, M.O. 2000. The biochemistry of apoptosis. *Nature.* 407:770–776.

Jiang, D., N. Jha, R. Boonplueang, and J.K. Andersen. 2001. Caspase 3 inhibition attenuates hydrogen peroxide-induced DNA fragmentation but not cell death in neuronal PC12 cells. *J. Neurochem.* 76:1745–1755.

Jurgensmeier, J.M., S. Krajewski, R.C. Armstrong, G.M. Wilson, T. Oltersdorf, L.C. Fritz, J.C. Reed, and S. Ottilie. 1997. Bax- and Bak-induced cell death in the fission yeast *Schizosaccharomyces pombe*. *Mol. Biol. Cell.* 8:325–339.

Kanduc, D., A. Mittelman, R. Serpico, E. Sinigaglia, A.A. Sinha, C. Natale, R. Santacroce, M.G. Di Corcia, A. Lucchese, L. Dini, et al. 2002. Cell death: apoptosis versus necrosis (review). *Int. J. Oncol.* 21:165–170.

Lesuisse, C., and L.J. Martin. 2002. Immature and mature cortical neurons engage different apoptotic mechanisms involving caspase-3 and the mitogen-activated protein kinase pathway. *J. Cereb. Blood Flow Metab.* 22:935–950.

Levkovitz, Y., and J.M. Baraban. 2002. A dominant negative Egr inhibitor blocks nerve growth factor-induced neurite outgrowth by suppressing c-Jun activation: role of an Egr/c-Jun complex. *J. Neurosci.* 22:3845–3854.

Maher, P., and D. Schubert. 2000. Signaling by reactive oxygen species in the nervous system. *Cell. Mol. Life Sci.* 57:1287–1305.

Majno, G., and I. Joris. 1995. Apoptosis, oncosis, and necrosis. An overview of cell death. *Am. J. Pathol.* 146:3–15.

Mansour, S.J., J.M. Candia, J.E. Matsuura, M.C. Manning, and N.G. Ahn. 1996. Interdependent domains controlling the enzymatic activity of mitogen-activated protein kinase kinase 1. *Biochemistry.* 35:15529–15536.

Martin, L.J. 2001. Neuronal cell death in nervous system development, disease, and injury (Review). *Int. J. Mol. Med.* 7:455–478.

Mazzoni, I.E., F.A. Said, R. Aloyz, F.D. Miller, and D. Kaplan. 1999. Ras regulates sympathetic neuron survival by suppressing the p53-mediated cell death pathway. *J. Neurosci.* 19:9716–9727.

Miller, T.M., and E.M. Johnson, Jr. 1996. Metabolic and genetic analyses of apoptosis in potassium/serum-deprived rat cerebellar granule cells. *J. Neurosci.* 16:7487–7495.

Miller, T.M., K.L. Moulder, C.M. Knudson, D.J. Creedon, M. Deshmukh, S.J. Korsmeyer, and E.M. Johnson, Jr. 1997a. Bax deletion further orders the cell death pathway in cerebellar granule cells and suggests a caspase-independent pathway to cell death. *J. Cell Biol.* 139:205–217.

Miller, T.M., M.G. Tansey, E.M. Johnson, Jr., and D.J. Creedon. 1997b. Inhibition of phosphatidylinositol 3-kinase activity blocks depolarization- and insulin-like growth factor I-mediated survival of cerebellar granule cells. *J. Biol. Chem.* 272:9847–9853.

Namura, S., K. Iihara, S. Takami, I. Nagata, H. Kikuchi, K. Matsushita, M.A. Moskowitz, J.V. Bonventre, and A. Alessandrini. 2001. Intravenous administration of MEK inhibitor U0126 affords brain protection against forebrain ischemia and focal cerebral ischemia. *Proc. Natl. Acad. Sci. USA.* 98:11569–11574.

Nicholson, D.W., A. Ali, N.A. Thornberry, J.P. Vaillancourt, C.K. Ding, M. Gallant, Y. Gareau, P.R. Griffin, M. Labelle, and Y.A. Lazebnik. 1995. Identification and inhibition of the ICE/CED-3 protease necessary for mammalian apoptosis. *Nature.* 376:37–43.

Nijhawan, D., N. Honarpour, and X. Wang. 2000. Apoptosis in neural development and disease. *Annu. Rev. Neurosci.* 23:73–87.

Noshita, N., T. Sugawara, T. Hayashi, A. Lewen, G. Omar, and P.H. Chan. 2002. Copper/zinc superoxide dismutase attenuates neuronal cell death by preventing extracellular signal-regulated kinase activation after transient focal cerebral ischemia in mice. *J. Neurosci.* 22:7923–7930.

Oppenheim, R.W. 1991. Cell death during development of the nervous system. *Annu. Rev. Neurosci.* 14:453–501.

Perry, G., H. Roder, A. Nunomura, A. Takeda, A.L. Friedlich, X. Zhu, A.K. Raina, N. Holbrook, S.L. Siedlak, P.L. Harris, and M.A. Smith. 1999. Activation of neuronal extracellular receptor kinase (ERK) in Alzheimer disease links oxidative stress to abnormal phosphorylation. *Neuroreport.* 10:2411–2415.

Pilar, G., and L. Landmesser. 1976. Ultrastructural differences during embryonic cell death in normal and peripherally deprived ciliary ganglia. *J. Cell Biol.* 68: 339–356.

Pulverer, B.J., J.M. Kyriakis, J. Avruch, E. Nikolakaki, and J.R. Woodgett. 1991. Phosphorylation of c-jun mediated by MAP kinases. *Nature.* 353:670–674.

Reiser, V., G. Ammerer, and H. Ruis. 1999. Nucleocytoplasmic traffic of MAP kinases. *Gene Expr.* 7:247–254.

Schulz, J.B., M. Weller, and T. Klockgether. 1996. Potassium deprivation-induced apoptosis of cerebellar granule neurons: a sequential requirement for new mRNA and protein synthesis, ICE-like protease activity, and reactive oxygen species. *J. Neurosci.* 16:4696–4706.

Shalin, S.C., U. Zirrgiebel, K.J. Honsa, J.P. Julien, F.D. Miller, D.R. Kaplan, and J.D. Sweatt. 2004. Neuronal MEK is important for normal fear conditioning in mice. *J. Neurosci. Res.* 75:760–770.

Sloviter, R.S. 2002. Apoptosis: a guide for the perplexed. *Trends Pharmacol. Sci.* 23:19–24.

Sperandio, S., I. de Belle, and D.E. Bredesen. 2000. An alternative, nonapoptotic

form of programmed cell death. *Proc. Natl. Acad. Sci. USA.* 97:14376–14381.

Stanciu, M., Y. Wang, R. Kentor, N. Burke, S. Watkins, G. Kress, I. Reynolds, E. Klann, M.R. Angiolieri, J.W. Johnson, and D.B. DeFranco. 2000. Persistent activation of ERK contributes to glutamate-induced oxidative toxicity in a neuronal cell line and primary cortical neuron cultures. *J. Biol. Chem.* 275: 12200–12206.

Subramaniam, S., J. Strelau, and K. Unsicker. 2003. Growth differentiation factor-15 prevents low potassium-induced cell death of cerebellar granule neurons by differential regulation of Akt and ERK pathways. *J. Biol. Chem.* 278: 8904–8912.

Vaux, D.L. 1993. Toward an understanding of the molecular mechanisms of physiological cell death. *Proc. Natl. Acad. Sci. USA.* 90:786–789.

Verdaguer, E., E. Garcia-Jorda, A. Jimenez, A. Stranges, F.X. Sureda, A.M. Canudas, E. Escubedo, J. Camarasa, M. Pallas, and A. Camins. 2002. Kainic acid-induced neuronal cell death in cerebellar granule cells is not prevented by caspase inhibitors. *Br. J. Pharmacol.* 135:1297–1307.

Wang, K.K. 2000. Calpain and caspase: can you tell the difference? *Trends Neurosci.* 23:20–26.

Wang, X., J.L. Martindale, Y. Liu, and N.J. Holbrook. 1998. The cellular response to oxidative stress: influences of mitogen-activated protein kinase signalling pathways on cell survival. *Biochem. J.* 333(Pt 2):291–300.

Watson, A., A. Eilers, D. Lallemand, J. Kyriakis, L.L. Rubin, and J. Ham. 1998. Phosphorylation of c-Jun is necessary for apoptosis induced by survival signal withdrawal in cerebellar granule neurons. *J. Neurosci.* 18:751–762.

Xia, Z., M. Dickens, J. Raingeaud, R.J. Davis, and M.E. Greenberg. 1995. Opposing effects of ERK and JNK-p38 MAP kinases on apoptosis. *Science.* 270: 1326–1331.

Zhu, J.H., S.M. Kulich, T.D. Oury, and C.T. Chu. 2002. Cytoplasmic aggregates of phosphorylated extracellular signal-regulated protein kinases in Lewy body diseases. *Am. J. Pathol.* 161:2087–2098.